Magnetic Steering of Superparamagnetic Nanoparticles in Duct Flow for Molecular Communication: A Feasibility Study

Niklas Schlechtweg[1], Sebastian Meyer[1], Harald Unterweger[2], Max Bartunik[1], Doaa Ahmed[1], Wayan Wicke[3], Vahid Jamali[3], Christoph Alexiou[2], Georg Fischer[1], Robert Weigel[1], Robert Schober[3], and Jens Kirchner[1(✉)]

[1] Institute for Electronics Engineering, Friedrich-Alexander-University Erlangen-Nürnberg, 91 058 Erlangen, Germany
jens.kirchner@fau.de
[2] Section for Experimental Oncology and Nanomedicine, University Hospital Erlangen, 91 052 Erlangen, Germany
[3] Institute for Digital Communications, Friedrich-Alexander-University Erlangen-Nürnberg, 91 058 Erlangen, Germany
https://lte.techfak.uni-erlangen.de/
http://www.hno-klinik.uk-erlangen.de/seon-nanomedizin/
https://www.idc.tf.fau.de/

Abstract. Molecular communication (MC) denotes information transmission by use of molecules and nanosized particles. For the realization of testbeds, superparamagnetic iron oxide nanoparticles (SPIONs) in duct flow have recently been proposed. Here, an experimental setup is provided to direct these particles at a branching of a tube into a specific direction by use of magnetic fields.

For that purpose, gold-coated SPIONs suspended in water at constant flow rate are considered at a Y-shaped connector of tubes. The particles are attracted by use of a custom-made electromagnet, while change of particle concentration in either of the branches is measured by a commercial susceptometer. The approach is evaluated for different flow rates and with the electromagnet both at a fixed position and moving along the tube. Exemplary measurements show that an information transmission is feasible in both approaches and with all tested flow rates.

The feasibility study hence shows that particle steering by use of magnetic fields is a viable approach, which is even robust against flow rate variations. It can thus be used in MC to address different transmission channels as well as to realize differential signal transmission. Furthermore, it might help to improve magnetic drug targeting in future applications.

Supported in part by the Friedrich-Alexander University Erlangen-Nürnberg (FAU) under the Emerging Fields Initiative (EFI), and the STAEDTLER Foundation.

L. Mucchi et al. (Eds.): BODYNETS 2019, LNICST 297, pp. 161–174, 2019.
https://doi.org/10.1007/978-3-030-34833-5_14

Keywords: Superparamagnetic nanoparticles · Particle steering · Magnetic field · Duct flow · Molecular communication

1 Introduction

Molecular communication (MC) encodes and transmits information in the concentration, type or structure of molecules or nanosized particles [9,20]. It thus provides an alternative to conventional electromagnetic- (EM-) based communication on small scale and in applications where EM energy is highly absorbed, e.g. in water and water solutions [6].

To this day, extensive theoretical and simulation-based investigations have been performed that improve the channel modeling in MC systems [1,2,13,14, 27]. In addition to the theoretical work, several experimental setups have been recently proposed [7,8,11,17,18]. These testbeds allow to put theoretical channel models to the test, identify and study the relevant physical processes involved and predict opportunities and limits of future realizations. The first such MC testbed was proposed by Farsad et al. [8], where alcohol is ejected by a nozzle through open air and detected by a sensor at variable distances between 2 and 4 m from the transmitter. The testbed was later extended to MIMO communication by use of two nozzles and two sensors as senders and receivers, respectively [17]. As an alternative approach, Farsad et al. [7] proposed to code information in the pH-level of a fluid by using two complementary pumps, which inject either an acid or a base into the main flow of tube, in order to transmit a bit 0 and 1, respectively, over a length of several decimeters.

Besides the pioneering work of N. Farsad et al., other air-based MC system concepts have been proposed since then [15]. Giannoukus et al. [10] designed an odor emitter, which uses a controlled evaporation of liquid chemicals and carrier gas such as nitrogen; Kennedy et al. [16,22] proposed the transmission and detection of concentration of isopropyl (IPA) alcohol vapor.

While alcohol- and pH-based demonstrators cannot be used for MC in humans, superparamagnetic iron oxide nanoparticles (SPIONs), which were originally developed for cancer therapy and are therefore biocompatible, could fill this gap. A corresponding testbed was presented by the authors [23]. Here, a peristaltic pump allows to inject a suspension of SPIONs into a constant background flow. After a few centimeters, these particles are detected by a susceptometer, which measures the change of inductance of a coil wound around the propagation channel. As a realization of on-off keying, a bit 1 is represented by a particle injection, a bit 0 by no injection.

However, all of the above mentioned approaches, irrespective of the signaling molecules under investigation, make use of mechanical pumps. Due to this very mode of operation, the pumps are limited in speed and granularity of the injected volumes. Furthermore, miniaturization of the testbeds will make these approaches inapplicable and will therefore call for alternatives.

For modulation of pH level, a replacement for the macroscopic pumps has already been proposed by Grebenstein et al. [11], based on Escherichia coli bacteria that, when stimulated by light pulses, emit protons and thus reduce the

local pH-level. Another modulator, appropriate for receiver design, was proposed in [18], where a specific signal molecule induces a fluorescence reaction in E. coli bacteria and thus allows interfacing chemical with optical and, by use of a photodetector, electrical domain. For modulation of SPIONs concentration, in contrast, no such alternative has been proposed so far.

In this paper we propose to make use of the superparamagnetic property of the nanoparticles in a tube system. We demonstrate that it is possible to direct the SPIONs into a particular channel at a Y-shaped branching of the tube system, overcoming the counteracting background flow in the tube system. Therefore we display a customized electromagnet that is utilized as steering unit.

For that purpose, the following sections will outline the fundamentals of the particle steering and describe the experimental setup. The results section will provide the first measurements, which demonstrate the feasibility of the approach. A summary of potential applications and future steps of research will conclude the article.

2 Fundamentals

2.1 Generation of Magnetic Fields

In order to steer the SPIONs by use of magnetic fields, an electromagnet is used. The underlying physical principles are formed in the Maxwell's equations, more accurate in Ampère's law. This partial differential equation describes the creation of a magnetic field of intensity $\boldsymbol{H}$ by a surface current density $\boldsymbol{J}$. Adding the displacement current density $\boldsymbol{D}$ as Maxwell's fixture to the equation, Ampère's law can be written as follows [12]:

$$\nabla \times \boldsymbol{H} = \boldsymbol{J} + \frac{\partial \boldsymbol{D}}{\partial t} \tag{1}$$

In magnetostatics currents are steady and the surrounding electric field is constant[1]. These conditions form a special case of Ampère's law [12]:

$$\frac{\partial \boldsymbol{D}}{\partial t} = 0$$

$$\nabla \times \boldsymbol{H} = \boldsymbol{J} \tag{2}$$

Using Stoke's theorem, Eq. (2) can be transformed from differential to integral form:

$$\oint_{\partial A} \boldsymbol{H}\, \mathrm{d}\boldsymbol{l} = \int_{A} \boldsymbol{J}\, \mathrm{d}\boldsymbol{A} = I \tag{3}$$

Equation (3) states that the total current I through a given surface A agrees with the circulation of $\boldsymbol{H}$ around A, i.e., the integral of $\boldsymbol{H}$ along the boundary of A. It can be rewritten in the form of the Biot-Savart law [12]

$$\mathrm{d}\boldsymbol{H}(\boldsymbol{r}) = \frac{I}{4\pi} \frac{\mathrm{d}\boldsymbol{l} \times (\boldsymbol{r} - \boldsymbol{l})}{\|\boldsymbol{r} - \boldsymbol{l}\|^2}, \tag{4}$$

[1] $\boldsymbol{D} = \varepsilon \boldsymbol{E}$ is known as constitutive relation with the electric field $\boldsymbol{E}$ and the relative permittivity ε.

which specifies the contribution $\mathrm{d}\boldsymbol{H}$ to the magnetic field intensity $\boldsymbol{H}$ at point $\boldsymbol{r}$ caused by an infinitesimal piece of wire $\mathrm{d}\boldsymbol{l}$ at position $\boldsymbol{l}$ that carries a current I.

Integration of (4) along a path $\mathrm{d}\boldsymbol{l}$ allows to determine the magnetic field caused by any current-carrying conductor in general and by an electric coil in particular. Analytical solutions can be derived for simple setups (see, e.g. [3,4,19]), whereas for the study of more complex electromagnets, particularly including core materials, simulation-based approaches are required.

In order to guide the magnetic flux and to increase the magnetic field outside the coil, cores of ferro- or ferrimagnetic materials such as iron are often used. In such magnetic media, an external field $\boldsymbol{H}$ induces a magnetization

$$\boldsymbol{M} = \chi \boldsymbol{H}, \tag{5}$$

which is proportional to the external field $\boldsymbol{H}$, with the material-dependent magnetic susceptibility χ as proportionality factor. The magnetic induction

$$\boldsymbol{B} = \mu_0(\boldsymbol{H} + \boldsymbol{M}) = \mu_0(1 + \chi)\boldsymbol{H} \tag{6}$$

is then composed of the external field and the magnetization of the material, where $\mu_0 = 4\pi \times 10^{-7}\mathrm{N/A}^2$ is the vacuum permeability.

Depending on the atomic structure of the material, the magnetization aligns against or with the external field, i.e., $\chi < 0$ and $\chi > 0$, respectively. The corresponding materials are denoted as diamagnetic ($\chi < 0$), paramagnetic ($\chi > 0$) and ferromagnetic ($\chi \gg 0$).[2] It is important to note that paramagnetic media do not exhibit remanent magnetization when the external field is turned off, whereas ferromagnetic media do so.

2.2 Superparamagnetic Iron Oxide Nanoparticles

While control of particles within the body by use of magnetic fields is highly desirable, e.g., for drug targeting, neither dia- nor paramagnetic materials could serve this purpose, due to a too low χ-value and therefore negligible reaction to the external magnetic field. Ferromagnetic materials are also not suitable due to the residual magnetization, which boosts agglomeration of the particles in the blood vessels and thus involves a high risk of vascular occlusion.

Superparamagnetic nanoparticles, in contrast, unite the benefits of para- and ferromagnetism. They are made of ferromagnetic material, usually from the iron oxides magnetite or maghemite (then called superparamagnetic iron oxide nanoparticles or short SPIONs), at sizes in the nanometer-range, typically between 10 nm and 100 nm. Due to these small dimensions, the particles do not exhibit remanence, while still offering high susceptibility values. Furthermore, SPIONs are biocompatible and thus applicable for human use. These nanoparticles have therefore been proposed and are investigated for use as diagnostic agents in magnetic resonance imaging and as non-viral gene vectors as well as for cancer therapy by drug targeting and magnetic hyperthermia [5,25].

[2] For the sake of simplicity, ferri- and antiferromagnetic materials are neglected here.

2.3 Particle Steering

In order to direct SPIONs into a specific direction from outside the body, an external magnetic field $\boldsymbol{B}$ is applied. Then a particle of volume V_P and susceptibility χ_P within a solution of susceptibility χ_S will be subject to the force [21,24]

$$\boldsymbol{F} = \frac{\chi_\mathrm{P} - \chi_\mathrm{S}}{\mu_0} V_\mathrm{P} \left(\boldsymbol{B} \cdot \boldsymbol{\nabla}\right) \boldsymbol{B}, \tag{7}$$

where $\boldsymbol{\nabla B}$ denotes the covariant derivative of $\boldsymbol{B}$, i.e., a tensor of degree 2.

From (7), it follows that $\boldsymbol{F}$ is proportional to the susceptibility of the particle relative to that of the solution, to the volume of the particle, to the strength of the magnetic field and to its gradient. While the former two factors are determined by the application scenario and the manufacturing of the SPIONs, the latter two factors depend on the design of the electromagnet and its position to the particle.

3 Methods

Based on the fundamentals introduced in the previous section, a demonstrator with a customized steering unit for the SPIONs has been developed. In Sect. 3.1 the proposed demonstrator is described in detail. In Sect. 3.2 different settings for the measurements will be introduced.

3.1 Measurement Setup

The setup in Fig. 1a shows a closed-loop flow of a suspension of nanoparticles in distilled water. From a reservoir, the particle suspension flows to the central part of the loop, a Y-shaped connector, which splits the tube into two branches (see also Fig. 1b). Through these branches, the particles flow back to the reservoir, where they can start the next flow cycle. The constant flow is driven by the peristaltic pump REGLO Digital (Ismatec, Wertheim, Germany), which is positioned at the end of the two branches before these enter the reservoir, which assures a symmetric flow in both branches. All tubes used have diameter of 1.5 mm. In order to steadily monitor the particle concentration in one branch of the tube, this branch leads through the detector coil of the susceptometer MS2G (Bartington Instruments, Witney, United Kingdom).

The setup can be regarded as transmission line between a transmitter located at the Y-connector and the susceptometer as receiver. A binary “1” is sent, when an increased particle concentration is induced by the transmitter via magnetic particle steering and measured at the receiver, a binary “0”, when a decreased particle concentration is induced. The setup hence forms a single-ended communication line; if the susceptometer is replace by a detector that contemporaneously measures both branches of the Y-connector and by that determines the concentration difference between the two branches, differential signal transmission is obtained.

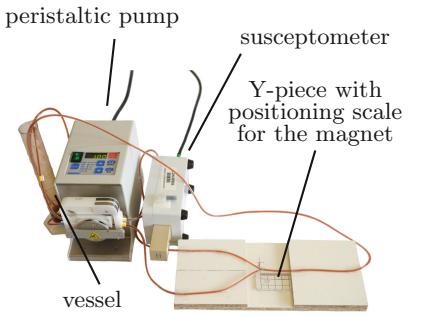

(a) Measurement setup to steer the SPIONs at the Y-shaped branching, to allow measuring the concentration in the desired tube.

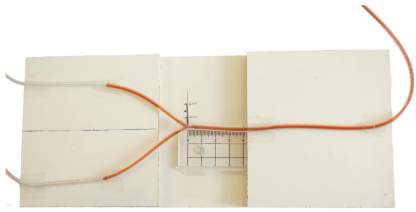

(b) Y-piece (close-up) with identical flow in both tubes.

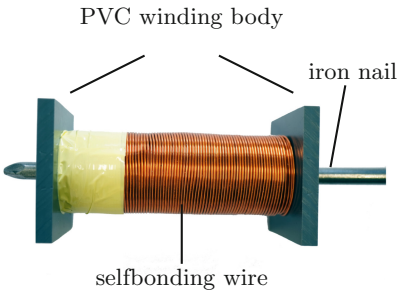

(c) Electromagnet used as a steering unit.

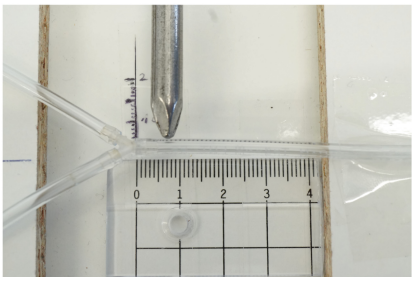

(d) Measurement with the electromagnet in a fixed position. The scaling parallel to the tube defines the x-coordinate, the scaling parallel to the nail defines the y-coordinate of the pointed end of the iron nail.

Fig. 1. Measurement setup.

The electromagnet displayed in Fig. 1c was specially designed as a steering unit for the demonstrator. The winding body was made of a polyvinyl chloride (PVC) tube with a length of 10 cm, an inner diameter of 7 mm and an outer diameter of 12 mm. Two additional PVC plates were mounted to the ends of the tube, to create axial limits for the windings. A selfbonding wire made out of copper with a diameter of 0.9 mm was coiled around the winding in 10 layers of 85 windings each, leading to a total winding number of 851. An iron nail with a length of 21 cm and a diameter of 7 mm was inserted into the winding body acting as core material, as well as focus for the magnetic flux density at the pointed end.

The magnet was operated at a voltage of 4.6 V and a current of 2.5 A max. ($P = 11.5$ W). The control measurement with an FM 302 magnetometer (Projekt Elektronik GmbH, Berlin, Germany) resulted in a magnetic flux density of 200 mT at the pointed end of the nail.

3.2 Measurement

For all the following test settings a new type of SPIONs, provided by the Section for Experimental Oncology and Nanomedicine (SEON) of the University Hospital Erlangen was used. These particles are coated with a golden layer. In Table 1 the parameters of the particles are listed.

Table 1. Parameters of the golden-layered particles (SPIONs).

Parameter	Value
Particle radius	424 nm
Iron concentration	1.12 mg/L
Gold concentration	0.27 mg/L

In Fig. 1d the pointed end of the nail is shown in a fixed position. Behind the tube a cartesian coordinate system is marking the position of the pointed end. Three series of measurements were performed, each with four measurement at different flow rates Q, where Q increased from 4 mL/min to 7 mL/min in steps of 1 mL/min. In each measurement the bit sequence [1, 1, 1, 1, 1, 1] of six consecutive "1" was sent, with a symbol duration of 20 s and a duty cycle of 5 s.

In the first two measurement series, during these 5 s the tip of the electromagnet was moved from point $A(x = 0; y = 0)$ to $B(x = 4; y = 0)$ following the scaling described in Fig. 1d alongside the tube, whereas during the remaining 15 s no magnetic force was exerted on the particle. In the first measurement series, the susceptibility was measured in the branch opposed to the magnet, i.e., in the branch where a decreased susceptibility is expected. In the second measurement series, the susceptometer was positioned around the branch on the same side as the magnet, i.e., the tube where an increase of susceptibility is expected. In the last measurement series, the electromagnet was fixed on position $A(x = 0; y = 0)$ and the tube with the decreasing susceptibility was measured.

3.3 Flow Profile

The efficiency of the particle steering with the setup described beforehand is highly dependent on the balance between the flow profile in the tube, the flow rate of the particles and the applied magnetic field. With the tube diameter of 1.5 mm and the flow rates stated above, it can be shown that the flow follows

a laminar flow profile [23,26], which is characterized by the parabolic velocity profile

$$v(r) = v_0 \left[1 - \left(\frac{r}{R}\right)^2\right], \tag{8}$$

where r is the radial coordinate, R the radius of the tube and v_0 the velocity of the particles at the center of the tube. This profile is illustrated in Fig. 2, which shows that the maximum velocity is present in the center of the tube cross section and decreases in radial direction towards the tube wall to zero.

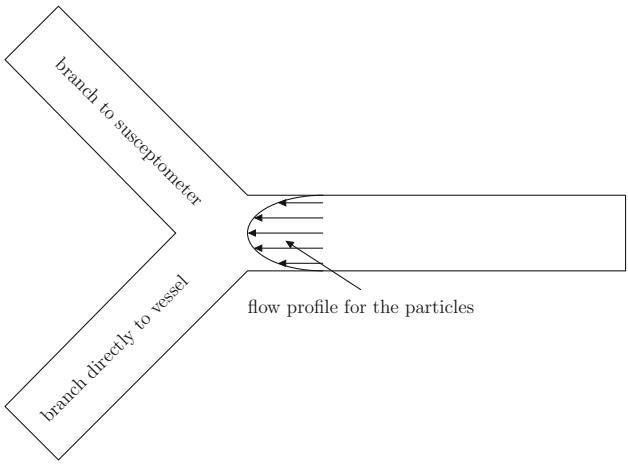

Fig. 2. Schematical illustration of the flow profile for the particles.

Relating the laminar flow profile to the particle concentration, it becomes clear that particles with a radial coordinate $r \approx R$ will stop moving. This means the particle steering unit not only directs the particles into the desired branch of the tube system, it can also force the particles from the tube borders to the center, thus from areas with low to higher velocity, and vice versa. Therefore the strength and position of the electromagnet affect the particle concentration that is lead into the desired branch.

4 Results

Figures 3, 4 and 5 display the results of the test settings described in the previous section. In each figure, the four subfigures show the susceptibility over time for the different flow rates given above. In addition to the raw measured signal, given in dark gray, the smoothed signal, computed by use of a moving average filter of width 5 s, is displayed in red color. The spacing of the abscissa is chosen such that it agrees with the symbol duration of 20 s.

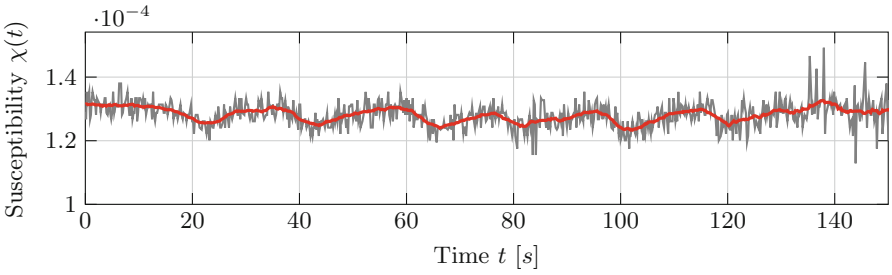

(a) $Q = 4\,\mathrm{mL/min}$

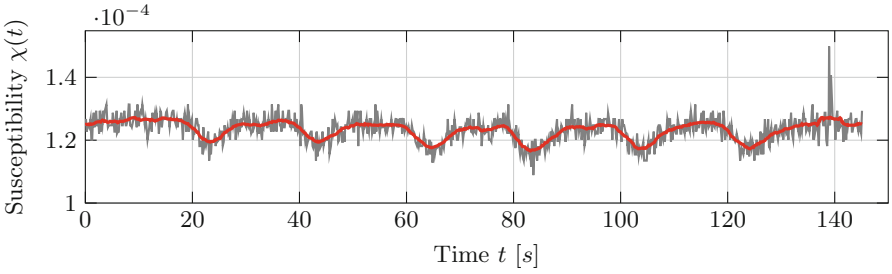

(b) $Q = 5\,\mathrm{mL/min}$

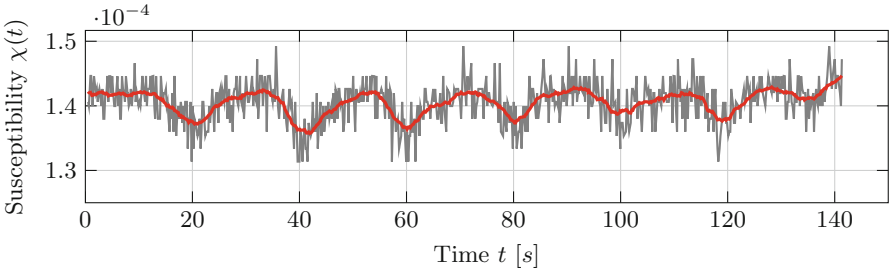

(c) $Q = 6\,\mathrm{mL/min}$

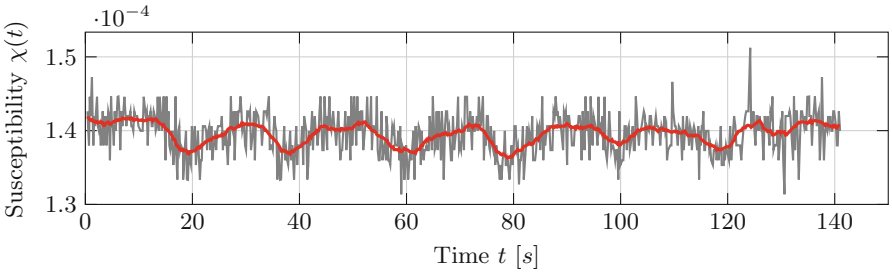

(d) $Q = 7\,\mathrm{mL/min}$

Fig. 3. Received signal due to a transmitted bit sequence for different flow rates Q with moving magnet and measuring the decreasing susceptibility; symbol duration $T = 20\,\mathrm{s}$; transmitted bit sequence: [1, 1, 1, 1, 1, 1]. Raw signal given in gray, smoothed signal in red color (moving average of with 5 s). (Color figure online)

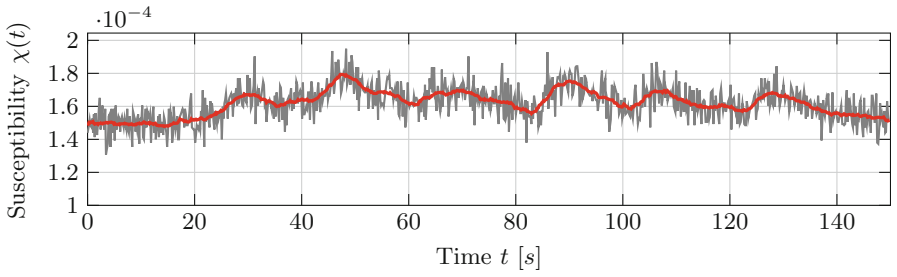

(a) $Q = 4\,\mathrm{mL/min}$

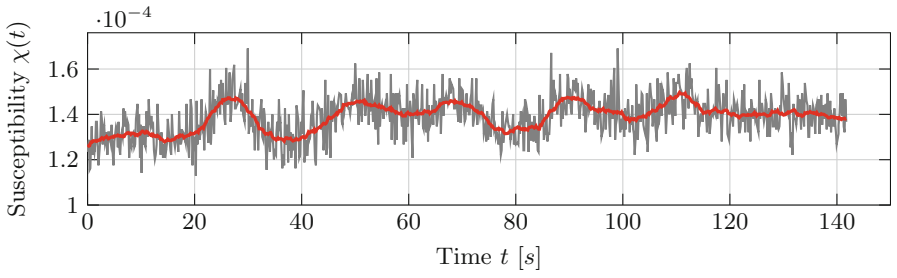

(b) $Q = 5\,\mathrm{mL/min}$

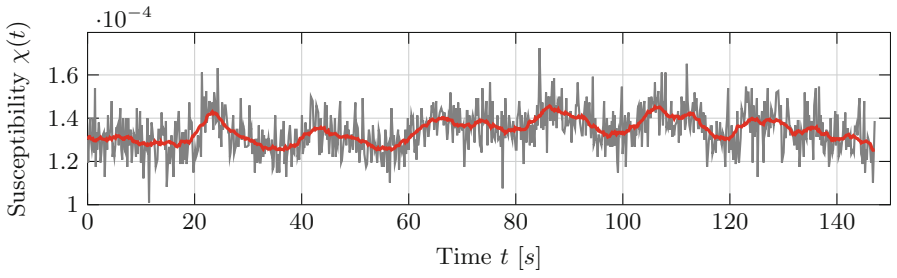

(c) $Q = 6\,\mathrm{mL/min}$

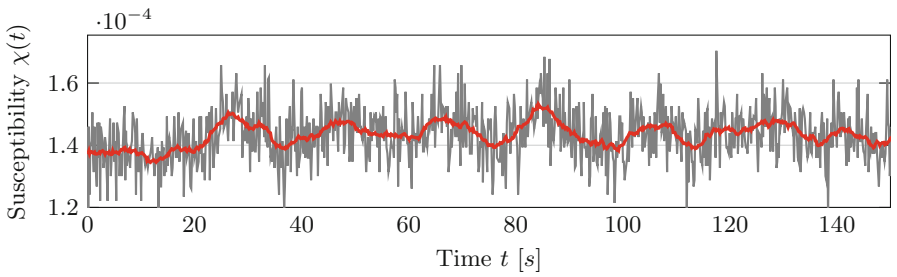

(d) $Q = 7\,\mathrm{mL/min}$

Fig. 4. Received signal due to a transmitted bit sequence for different flow rates Q with moving magnet and measuring the increasing susceptibility; symbol duration $T = 20\,\mathrm{s}$; transmitted bit sequence: [1, 1, 1, 1, 1, 1]. Raw signal given in gray, smoothed signal in red color (moving average of with 5 s). (Color figure online)

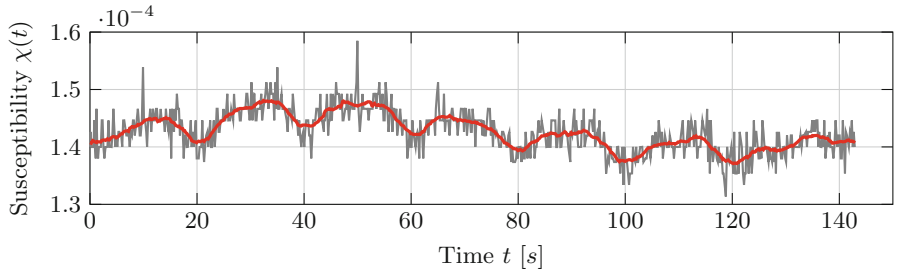

(a) $Q = 4\,\mathrm{mL/min}$

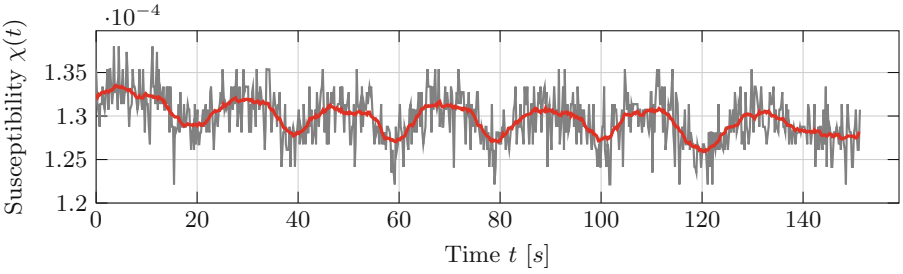

(b) $Q = 5\,\mathrm{mL/min}$

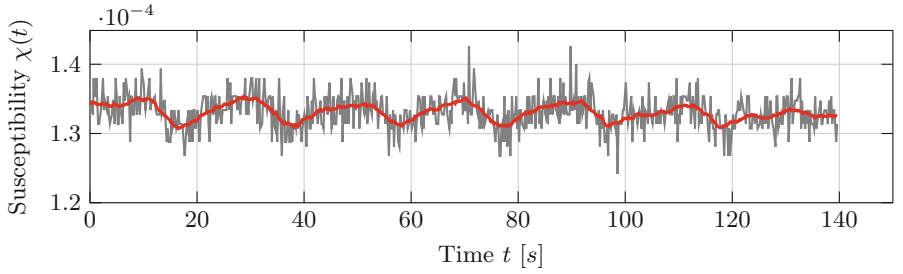

(c) $Q = 6\,\mathrm{mL/min}$

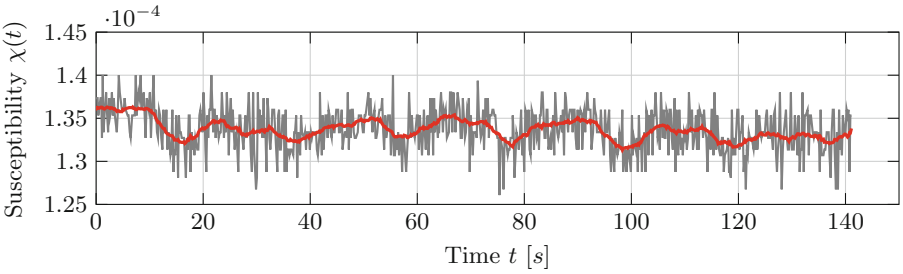

(d) $Q = 7\,\mathrm{mL/min}$

Fig. 5. Received signal due to a transmitted bit sequence for different flow rates Q with fixed magnet and measuring the decreasing susceptibility; symbol duration $T = 20\,\mathrm{s}$; transmitted bit sequence: [1, 1, 1, 1, 1, 1]. Raw signal given in gray, smoothed signal in red color (moving average of with 5 s). (Color figure online)

In each plot a periodic pattern of decrease or increase of the susceptibility, more precise the peaks that correspond to the transmitted bit sequence, are clearly visible. After the duty cycle, the susceptibility always returns to its baseline value. Note that the arrival time of the first peak depends on the flow rate.

Furthermore, the expectations concerning increase and decrease of the particle concentration are met. The branch opposite to the magnet leads exhibits indeed a reduction of the susceptibility, i.e., the magnet detracts the particle from this path (Fig. 3). In contrast, the branch on the same side as the magnet shows an increase in susceptibility, i.e., an accumulation of particles in this branch is observed (Fig. 4).

Due to the laminar flow in the tube, with the zero flow at its boundary, particles tend to get stuck at the surface of the tube wall, when no external magnetic field is operated. This leads to a lower overall particle concentration in both branches together and in the susceptometer in particular, in consequence decreasing peak amplitudes of the bit sequence. This behavior will pose a major challenge on magnetic particle steering and was addressed here in two approaches: by moving the magnet alongside the tube to direct the particles into the desired branch in the first two measurements, and by keeping the electromagnet at a fixed position in the third measurement. The results show that both approaches allow satisfactory transmission behavior. While the fixed-position approach would be easier to realize, an implementation comparable to the approach with the moving magnet, using a series of electromagnets along the tube instead, is possible, too.

The variation of the flow rates in the different setups proves a second thing: that information transmission in the proposed approach is feasible for different flow rates, i.e., it is robust against flow rate variations.

5 Conclusion

The measurements have shown that it is possible to steer superparamagnetic nanoparticles at a branching of a flow channel by use of magnetic fields in such a way that an accumulation of particles is observed in one channel and a diminution in the other. This steering is successful under different flow conditions. However, note that the approach is sensitive to the testbed parameters, viz. flow as well as position and strength of the electromagnet: If not properly balanced, the particles either are not sufficiently deflected or accumulate in front of the branching in the low-flow region of the tube close to the walls. Therefore, the next steps of research will include a simulation-based optimization of the setup, before the next realization of the testbed is tackled. Besides investigation of the said parameters, improvements of the steering unit might be obtained. Here, a second magnet could be added to create a channel switch function, as well as using more magnets alongside the tube, as was suggested in Sect. 4.

With an optimal setup for steering of SPIONs at channel branchings, several applications become possible: First of all, it can replace the original transmitter of the MC testbed described in [23] without the restrictions imposed by

mechanical devices. Then one of the branches would be used for signal transmission, while the other, unused branch would direct the particles into a waste bin. Second, in contrast to this single-ended approach, an MC testbed can be realized with differential signaling, i.e., where information is coded in the difference between two parallel tubes rather than in the absolute value of a single tube. In both of these scenarios, the particle steering module would be responsible for the modulation of the SPIONs concentration and thus be the central part of the receiver. It can play yet another role and, third, direct the particles into different channels before modulation takes place, such that different receivers can be addressed. Finally, it should be mentioned that the steering of SPIONs can provide a benefit beyond molecular communication, viz. in cancer therapy, where an optimized targeting of the tumor by drug-loaded nanoparticles could reduce medication dosage and thus side effects of chemotherapy.

References

1. Andrews, S.S.: Accurate particle-based simulation of adsorption, desorption and partial transmission. Phys. Biol. **6**(4), 046015 (2009). https://doi.org/10.1088/1478-3975/6/4/046015
2. Bicen, A.O., Akyildiz, I.F.: Molecular transport in microfluidic channels for flow-induced molecular communication. In: 2013 IEEE International Conference on Communications Workshops (ICC), pp. 766–770, June 2013. https://doi.org/10.1109/ICCW.2013.6649336
3. Dasgupta, B.B.: Magnetic field due to a solenoid. Am. J. Phys. **52**, 258 (1984)
4. Derby, N., Olbert, S.: Cylindrical magnets and ideal solenoids. Am. J. Phys. **78**, 228–235 (2010)
5. Dulińska-Litewka, J., Łazarczyk, A., Hałubiec, P., Szafrański, O., Karnas, K., Karewicz, A.: Superparamagnetic iron oxide nanoparticles–current and prospective medical applications. Materials **12**(4) (2019). https://doi.org/10.3390/ma12040617
6. Eremenko, Z.E., Kuznetsova, E.S., Shubnyi, A.I., Martunov, A.V.: High loss liquid in layered waveguide at microwaves and applications. In: 2018 IEEE 17th International Conference on Mathematical Methods in Electromagnetic Theory (MMET), pp. 246–249, July 2018. https://doi.org/10.1109/MMET.2018.8460267
7. Farsad, N., Pan, D., Goldsmith, A.: A novel experimental platform for in-vessel multi-chemical molecular communications. In: GLOBECOM 2017–2017 IEEE Global Communications Conference, pp. 1–6, December 2017. https://doi.org/10.1109/GLOCOM.2017.8255058
8. Farsad, N., Guo, W., Eckford, A.: Tabletop molecular communication: text messages through chemical signals. Public Libr. Sci. ONE **8**, e82935 (2013)
9. Farsad, N., Yilmaz, B., Eckford, A., Chae, C.B., Guo, W.: A comprehensive survey of recent advancements in molecular communications. IEEE Commun. Surv. Tutor. **18**, 1887–1919 (2016)
10. Giannoukos, S., Marshall, A., Taylor, S., Smith, J.: Molecular communication over gas stream channels using portable mass spectrometry. J. Am. Soc. Mass Spectrom. **28**(11), 2371–2383 (2017). https://doi.org/10.1007/s13361-017-1752-6
11. Grebenstein, L., et al.: Biological optical-to-chemical signal conversion interface: a small-scale modulator for molecular communications. IEEE Trans. Nanobiosci. **18**(1), 31–42 (2019). https://doi.org/10.1109/TNB.2018.2870910

12. Griffiths, D.J.: Introduction to Electrodynamics. Always Learning, 4th edn. Pearson, Boston (2013). International Edition
13. Gul, E., Atakan, B., Akan, O.B.: NanoNS: a nanoscale network simulator framework for molecular communications. Nano Commun. Netw. **1**(2), 138–156 (2010). https://doi.org/10.1016/j.nancom.2010.08.003. http://www.sciencedirect.com/science/article/pii/S1878778910000256
14. Iwasaki, S., Yang, J., Nakano, T.: A mathematical model of non-diffusion-based mobile molecular communication networks. IEEE Commun. Lett. **21**(9), 1969–1972 (2017). https://doi.org/10.1109/LCOMM.2017.2681061
15. Jamali, V., Ahmadzadeh, A., Wicke, W., Noel, A., Schober, R.: Channel modeling for diffusive molecular communication - a tutorial review. CoRR abs/1812.05492 (2018). http://arxiv.org/abs/1812.05492
16. Kennedy, E., Shakya, P., Ozmen, M., Rose, C., Rosenstein, J.K.: Spatiotemporal information preservation in turbulent vapor plumes. Appl. Phys. Lett. **112**(26), 264103 (2018). https://doi.org/10.1063/1.5037710
17. Koo, B., Lee, C., Yilmaz, H.B., Farsad, N., Eckford, A., Chae, C.: Molecular MIMO: from theory to prototype. IEEE J. Sel. Areas Commun. **34**(3), 600–614 (2016)
18. Krishnaswamy, B., et al.: Time-elapse communication: bacterial communication on a microfluidic chip. IEEE Trans. Commun. **61**(12), 5139–5151 (2013). https://doi.org/10.1109/TCOMM.2013.111013.130314
19. Labinac, V., Erceg, N., Kotnik-Karuza, D.: Magnetic field of a cylindrical coil. Am. J. Phys. **74**, 621–627 (2006)
20. Nakano, T., Eckford, A., Haraguchi, T.: Molecular Communication. Cambridge University Press, Cambridge (2013)
21. Rikken, R.S.M., Nolte, R.J.M., Maan, J.C., van Hest, J.C.M., Wilson, D.A., Christianen, P.C.M.: Manipulation of micro- and nanostructure motion with magnetic fields. Soft Matter **10**, 1295–1308 (2014)
22. Shakya, P., Kennedy, E., Rose, C., Rosenstein, J.K.: Correlated transmission and detection of concentration-modulated chemical vapor plumes. IEEE Sens. J. **18**(16), 6504–6509 (2018). https://doi.org/10.1109/JSEN.2018.2850150
23. Unterweger, H., et al.: Experimental molecular communication testbed based on magnetic nanoparticles in duct flow. In: 2018 IEEE 19th International Workshop on Signal Processing Advances in Wireless Communications (SPAWC), pp. 1–5, June 2018. https://doi.org/10.1109/SPAWC.2018.8446011
24. Urbach, A.R., Love, J.C., Prentiss, M.G., Whitesides, G.M.: Sub-100 nm confinement of magnetic nanoparticles using localized magnetic field gradients. J. Am. Chem. Soc. **125**(42), 12704–12705 (2003). https://doi.org/10.1021/ja0378308
25. Wahajuddin, S.A.: Superparamagnetic iron oxide nanoparticles: magnetic nanoplatforms as drug carriers. Int. J. Nanomed. **7**, 3445–3471 (2012). https://doi.org/10.2147/IJN.S30320
26. White, F.: Fluid Mechanics, 7th edn. McGraw-Hill, New York (2011)
27. Yilmaz, H.B., Suk, G., Chae, C.: Chemical propagation pattern for molecular communications. IEEE Wirel. Commun. Lett. **6**(2), 226–229 (2017). https://doi.org/10.1109/LWC.2017.2662689